agriculture

MDPI

Article

Transcriptomic and Metabolomic Analyses Reveal Differences in Flavonoid Synthesis During Fruit Development of *Capsicum frutescens pericarp*

Yinxin Yang [1], Qihang Cai [1], Xuan Wang [1], Yanbo Yang [1], Liping Li [2], Zhenghai Sun [1,*] and Weiwei Li [3]

[1] Yunnan International Joint R&D Center for Intergrated Utilization of Ornamental Grass, International Technological Cooperation Base of High Effective Economic Forestry Cultivating of Yunnan Province, South and Southeast Asia Joint R&D Center of Economic Forest Full Industry Chain of Yunnan Province, College of Landscape and Horticulture, Southwest Forestry University, Kunming 650224, China; yangyinxin@swfu.edu.cn (Y.Y.); caiqihang@swfu.edu.cn (Q.C.); wangxuan@swfu.edu.cn (X.W.); yang_yb@swfu.edu.cn (Y.Y.)

[2] College of Geography and Ecotourism, Southwest Forestry University, Kunming 650224, China; 420882556@swfu.edu.cn

[3] Yunnan International Joint Center of Urban Biodiversity, Kunming 650223, China; liweiwei@mail.kiz.cas.cn

* Correspondence: szh@swfu.edu.cn

Abstract: *Capsicum frutescens* is a valuable economic crop that is widely cultivated for its unique flavor and rich nutritional content. While some studies have shown differences in flavonoid content among different chili species, the mechanism by which changes in flavonoid composition lead to fruit color variations in *C. frutescens* remains underreported. We performed transcriptomics and widely targeted metabolome sequencing on three different growth stages of the *C. frutescens* fruit and analyzed the data to better understand the mechanism of color change. Based on previous research on the genes that regulate flavonoid compounds and the MBW complex, we have identified a total of 28 core genes related to flavonoid biosynthesis and 8 genes that may be related to flavonoid synthesis. Through extensive targeted metabolomic analysis, 581 differential metabolites were identified, including 43 flavonoids. Most anthocyanins, flavonols, and flavonoids were found to be more abundant during the immature fruit stage, which we presume is associated with the differential expression of genes involved in flavonoid biosynthesis and regulation. These findings provide a useful reference for understanding flavonoid synthesis and the accumulation of fruits in *C. frutescens*.

Keywords: *Capsicum frutescens*; flavonoids; transcriptome; metabolome

check for updates

Received: 16 December 2024
Revised: 17 January 2025
Accepted: 18 January 2025
Published: 20 January 2025

Citation: Yang, Y.; Cai, Q.; Wang, X.; Yang, Y.; Li, L.; Sun, Z.; Li, W. Transcriptomic and Metabolomic Analyses Reveal Differences in Flavonoid Synthesis During Fruit Development of *Capsicum frutescens pericarp*. *Agriculture* **2025**, *15*, 222. https://doi.org/10.3390/agriculture15020222

Copyright: © 2025 by the authors. Licensee MDPI, Basel, Switzerland. This article is an open access article distributed under the terms and conditions of the Creative Commons Attribution (CC BY) license (https://creativecommons.org/licenses/by/4.0/).

1. Introduction

The color of chili fruits changes as they grow, which is an interesting phenomenon. People often judge whether the fruit is ripe or not by color change. The mechanism of fruit color change has long concerned breeders and consumers [1]. A beautiful fruit color can often significantly increase the economic value of the crop [2]. Previous studies have shown that chili fruit color is primarily associated with flavonoids, carotenoids, and chlorophyll [3]. Flavonoids, as important secondary metabolites, are widely distributed in plants. Thanks to technological progress, about 9000 flavonoids in plants have been identified [4]. These compounds shared a core structure consisting of 15 carbon atoms and could be categorized into six major classes based on molecular structure: flavonols, flavanones, flavones, isoflavones, catechins, and anthocyanins [5].

The synthesis of flavonoid compounds is initiated by phenylalanine (L-phenylalanine) through the phenylpropanoid and flavonoid pathways. In the phenylpropanoid pathway, phenylalanine is catalyzed by three key enzymes: phenylalanine ammonia-lyase (*PAL*), 4-coumarate-CoA ligase (*4CL*), and cinnamate-4-hydroxylase (*C4H*) to form p-coumaroyl-CoA [6]. This compound serves as the precursor for flavonoid biosynthesis. Through the action of chalcone synthase (*CHS*) and chalcone isomerase (*CHI*), naringenin is synthesized from p-coumaroyl-CoA [7]. Naringenin is a critical intermediate in the flavonoid biosynthetic pathway, undergoing a series of enzymatic reactions to form various types of flavonoid compounds. Flavonoids, which are polyphenolic substances, play crucial roles in plant physiological processes, including plant–animal interactions, attracting pollinators, protecting against ultraviolet (UV) damage, and contributing to the pigmentation of plant organs [4,8]. In addition to structural genes, transcription factors have been reported to regulate flavonoid biosynthesis by modulating the expression of flavonoid biosynthetic genes. For instance, basic helix–loop–helix (*bHLH*), WD repeat (*WD*), and *R2R3 MYB* transcription factors, as well as MADS-box proteins, are involved in this regulation. Research by Koes et al. demonstrated that bHLH and WD proteins interact with *MYB* transcription factors to form the MBW complex (MYB–bHLH–WD repeat), which regulates flavonoid accumulation in plants [9]. Further studies on *Arabidopsis* have also confirmed a strong correlation between *MYB* transcription factors and flavonoid biosynthesis [10].

The fruit color of *C. frutescens* changes at different developmental stages. These changes are primarily due to the accumulation of flavonoids and carotenoids [11]. Anthocyanin biosynthesis mainly depends on the biosynthesis of flavonoids and is mainly accumulated in the pericarp of chili peppers. Research on anthocyanins has identified that *CaANT1*, *CaANT2*, *CaAN1*, and *CaTTG1* are involved in their accumulation, influencing fruit color variation [12]. Howard further reported significant differences in the accumulation of flavonoids and related metabolites in chili fruits across different developmental stages and environmental conditions [13].

Although some genes related to fruit color have been cloned in *C. frutescens*, the mechanisms by which these genes regulate flavonoid accumulation and influence fruit color changes are still underreported. While fruit color is recognized as a key quality trait in *C. frutescens*, most studies have focused on pigments such as chlorophyll and carotenoids. The large-scale identification and quantification of flavonoids in *C. frutescens* remains rare. In this study, we used extensive targeted metabolomics to detect and quantify flavonoids in the pericarp of *C. frutescens* based on the UPLC-MS/MS analysis platform and a self-built database. Eukaryotic transcriptomics was also used to sequence the *C. frutescens* pericarp tissue. By combining transcriptomics and metabolomics data, we identified the core genes involved in the synthesis of flavonoids in *C. frutescens* and potential candidate genes. These findings were validated by quantitative real-time PCR (qRT-PCR). Integrating multi-omics data revealed changes in flavonoid accumulation and corresponding gene expression levels during fruit color development. The results provide important insights into the regulation of fruit color in *C. frutescens* by flavonoid compounds.

2. Materials and Methods

2.1. C. frutescens Material Germination Treatment, Growth Conditions, and Management Methods

The seeds of *C. frutescens* were sourced from the laboratory at Southwest Forestry University (*C. frutescens* seeds are all diploid.). The *C. frutescens* seeds were rinsed in running water, soaked in distilled water at 50 °C for 15 min, and then left at room temperature for 24 h. The seeds were placed in a petri dish with the bottom lined with two layers of filter paper to keep them moist. The treated seeds were placed in an incubator at 25 °C until they germinated. Subsequently, they were sown in a peat and vermiculite mixture (3:1) and

transferred to 20 cm diameter pots. The plants were cultivated at the Southwest Forestry University growing base (longitude 102.454308°, latitude 25.035229°) at a temperature of 25 °C, with 60–70% relative humidity and a light regime of 16 h of light and 8 h of darkness. They were watered every five days to keep the soil moist, and the plants were not fertilized or pruned.

To investigate the potential mechanisms behind fruit color development, qRT-PCR was used to analyze the gene expression in the fruit peels of *C. frutescens* at 50, 65, and 80 days post-anthesis (Figure 1). The first stage (50 days post-anthesis) represents the early stage of fruit development, at which the fruits are fully green and the fruit expansion has ceased, referred to as the GR stage. The second stage (65 days post-anthesis) corresponds to the mid-development stage, during which the fruit turns fully orange, referred to as the OR stage. In the third stage (80 days post-anthesis), the fruit is fully matured and red, referred to as the RE stage. After cleaning the surface of the fruit with ddH_2O, the samples were flash-frozen in liquid nitrogen and stored at −80 °C for further analysis.

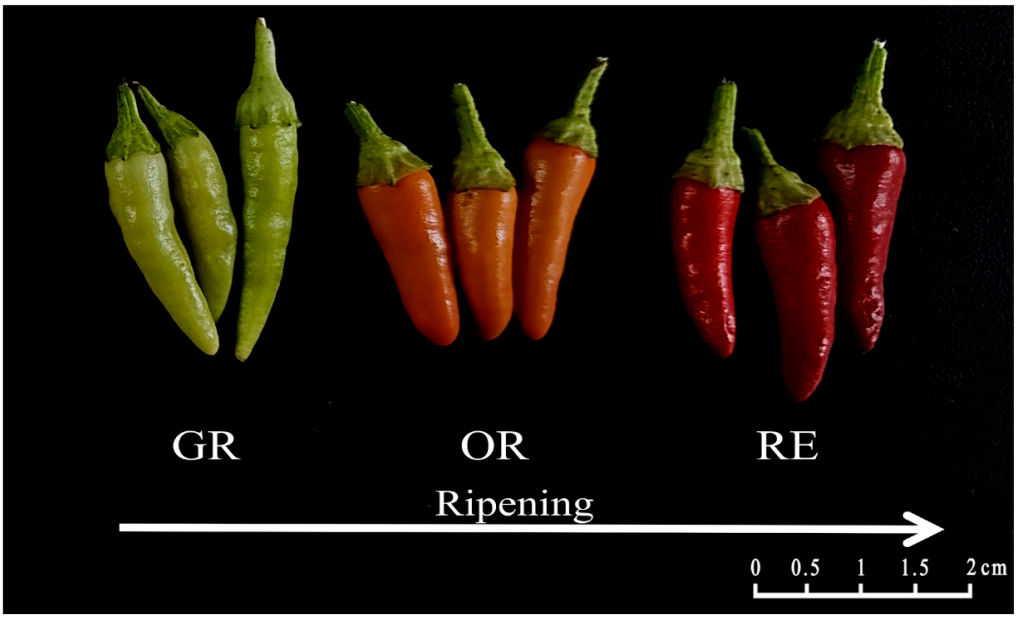


Figure 1. Developmental stages of *C. frutescens* used in this study. GR: Early fruit maturity stage (50 days post-anthesis); OR: Semi-mature stage (65 days post-anthesis); RE: Fully mature stage (80 days post-anthesis).

2.2. Sample Preparation and Extraction for Metabolite Analysis

Fruits of *C. frutescens* without pest or disease damage were collected at 50, 65, and 80 days post-anthesis. The fruit surfaces were rinsed with ddH_2O and rapidly frozen in liquid nitrogen, then stored at −80 °C. The sample was sent to Wuhan Metware Biotechnology Co., Ltd. (Wuhan, China) for the analysis of flavonoid compounds using a widely targeted metabolome analysis based on the UPLC-MS/MS detection platform and a self-built database. The chromatographic separation was carried out on an ACQUITY BEH C18 column (1.7 µm, 2.1 mm × 100 mm, Waters Technologies Co., Ltd., Milford, MA, USA). The mobile phase consisted of solvent A (0.1% formic acid in water) and solvent B (0.1% formic acid in acetonitrile). The elution gradient was as follows: 95% solvent A and 5% solvent B at the start, gradually changing to 5% solvent A and 95% solvent B over 9 min, holding for 1 min. The composition was then adjusted back to 95% solvent A and 5% solvent B over 60 s and maintained for 180 s. The flow rate was set to 0.35 mL/min, and the column temperature was maintained at 40 °C.

2.3. Differential Metabolites Analysis

An orthogonal partial least squares discriminant analysis (OPLS-DA) was performed using the OPLSR.Anal function in the R package Metabo Analyst R (Analysis package and version: R version 3.5.1; Basic analysis parameters: Default parameters). The data were log-transformed (log_2) and mean-centered prior to the OPLS-DA analysis. To avoid overfitting, permutation tests (200 permutations) were conducted. In the OPLS-DA analysis of *C. frutescens* fruit peel samples at different developmental stages, differential metabolites were identified based on VIP values (VIP > 1) and the absolute value of Log_2 fold change ($|Log_2FC| \geq 1$).

2.4. KEGG Annotation and Enrichment Analysis

Functional enrichment analysis is one of the most widely used techniques to reveal the application of gene sequences [14]. This study used the KEGG database to annotate the differential metabolites identified in the previous steps, following the method of Peng et al. [15] (http://www.kegg.jp/kegg/compound/; accessed on 5 March 2024). These annotated metabolites were then mapped to metabolic pathways in the KEGG Pathway database [16] (http://www.kegg.jp/kegg/pathway.html; accessed on 6 March 2024). The pathways containing significantly regulated metabolites were subjected to metabolite set enrichment analysis (MSEA), with the significance determined by *p*-values from hypergeometric tests.

2.5. Transcriptome Sequencing and Data Analysis

Total RNA was extracted from frozen peel samples of *C. frutescens* at different developmental stages using TRIzol® reagent (Thermo Fisher Scientific Inc., Waltham, MA, USA), following the manufacturer's instructions. The quality and quantity of total RNA extracted from the pericarp of *C. frutescens* were assessed using a Qubit fluorometer (Thermo Fisher Scientific Inc., Waltham, MA, USA) and a Qsep400 high-throughput biofragment analyzer (Vazyme Biotech Co., Ltd., Nanjing, China). For RNA sequencing, 1 µg of total RNA from each of the three developmental stages (with three biological replicates per stage) was used to construct sequencing libraries with the NEB Next® Ultra™ RNA Library Prep Kit for Illumina® (New England Biolabs, Inc., Ipswich, MA, USA). After library preparation, the concentration and fragment size were assessed using the Qubit fluorometer and Qsep400 analyzer, and the effective concentration of the library was quantified using qRT-PCR. Once quality control was passed, the libraries were pooled according to their effective concentrations and target sequencing output, and sequencing was performed on the Illumina platform in PE150 mode (2 × 150 bp). The reference genome for this study is Zhangshugang_genome.fa.gz (http://ted.bti.cornell.edu/ftp/pepper/genome/Zhangshugang/; accessed on 1 April 2024). The number of reads for each gene was obtained by comparing the results using featureCounts and statistical analysis [17]. Differential gene expression analysis between different biological conditions was performed using DESeq2 to obtain the set of differentially expressed genes between different biological conditions [18,19]. After differential analysis, the Benjamini–Hochberg method was used to correct the hypothesis test probability (*p* value) for multiple hypothesis testing and obtain the false discovery rate (FDR) [20]. The screening criteria for differentially expressed genes in this study were $|log_2\text{Fold Change}| \geq 1$ and FDR < 0.05.

2.6. qRT-PCR Validation of Candidate Genes

Based on comprehensive transcriptomics and metabolomics analyses of *C. frutescens*, we obtained a total of 8928 differentially expressed genes, among which we identified 23 genes highly related to flavonoids, including *CHS 1*, *CHS 2*, *HCT 2*, *HCT 3*, *E5.2.1.6 1*,

E5.2.1.6 2, *CYP73A 1*, *CYP73A 2*, *F3H 1*, *C3H 1*, *DFR 1*, *DFR 2*, *FLS 1*, *FLS 2*, and *CYP75B1 1*, along with transcription factors *MYB 15*, *MYB 16*, *MYB 61*, *bHLH 68*, *bHLH 3*, *bHLH 105*, *bHLH 13*, and *WD 40*. qRT-PCR technology was used to analyze the expression patterns of the abovementioned genes. Total RNA was extracted from peel tissues at different developmental stages using the FastPure® Plant Total RNA Isolation Kit (Vazyme Biotech Co., Ltd., Nanjing, China) and reverse-transcribed into cDNA using the All-In-One 5X RT MasterMix kit (Applied Biological Materials Inc., Shanghai, China). The Primer-BLAST tool from the NCBI database was used to design qRT-PCR primers (https://www.ncbi.nlm.nih.gov/; accessed on 20 June 2024) (Table 1). Relative gene expression was calculated using the $2^{-\Delta\Delta Ct}$ method using the UBI gene as an internal reference [21].

Table 1. Primer sequences used in this study.

Serial Number	Name	Gene ID	Forward Primer (5′→3′)	Reverse Primer (5′→3′)
1	HCT 2	Caz11g15030	GTTGGGAAGTTGTTGCCAGT	AGTGTCCATGAAAGGAGCAAC
2	E5.2.1.6 1	Caz11g20530	ACCACCTTGTTCCTTGCTGG	AGCAAGAAATGGAACGGCAC
3	E5.2.1.6 2	Caz05g17210	TTGAGGCTATTGTTAACGCTCC	ATAGCGCTCTCTAGCTGCAC
4	CYP73A 1	Caz06g02540	GGCCTTTCTTGAGGGGCTAC	AGCATTGCTGTCCATGCTCT
5	CYP73A 1	Caz06g02530	GTAACTGAGCCAGACACCCA	TTAGCCAACCACCAAGGGTT
6	F3H 1	Caz02g22300	CTTGGGCTGAAACGACACAC	AACGGGCTGAACAGTGATCC
7	C3′H 1	Caz10g22080	GGACAGTACTAAGCCTGGCAAT	GGTTTTCCAGCCATTTTAATCCCA
8	DFR 1	Caz12g17770	CAGGAGGAAGTGGTTATCTTGG	CACATCCCTTTTAAGGTCTGGATG
9	FLS 1	Caz01g28820	ACAGGGTAAAGGCAGCTCAG	TCTCCCGTTAGTTAGAACCTCAA
10	MYB 16	Caz02g29850	GGTCGATCTCCATGCTGTGA	TAATGCACGCCAGCTACCAT
11	MYB 15	Caz07g15260	TGGAAATAGGTGGTCGGCG	TGATTCATCACTTGAGTTTGTCGC
12	MYB 61	Caz08g15240	GGCTTCAGAATCAAACGCCG	GAATTGACCGAAGACGGCAG
13	bHLH 68	Caz03g02530	CAGCCTCCGTCTTGTCAGAA	CACAACCCTCTGCTCCTCAA
14	bHLH 3	Caz04g05400	AGGTGGACTCCCCATGCTAA	TCTCGTGCGATCGAGTAAGC
15	bHLH 105	Caz07g14570	TTCTCGGCCGTTTAGTTCCC	GAGGAGGCCGGTCAGAAAAG
16	bHLH 13	Caz11g13500	GCGTGGCATTTCCAAACCAA	CTGGAACGACGGAAGGTAGC
17	WD 40	Caz12g11340	AATACGCGTGTGGAAGTTGC	TACGCCACACCCGAATCTTACC
18	UBI3	Caz06g27840	GTCCATCTGCTCTCTGTTG	CACCCCAAGCACAATAAGAC

3. Results

3.1. Analysis of Pericarp Metabolomics Data of C. frutescens at Different Principal Growth Periods

3.1.1. PCA Analysis of Metabolomics Data of *C. frutescens* Peel at Different Growth Stages

A PCA was conducted to assess the differences between groups based on metabolomics data. The PCA results showed that PC1 and PC2 accounted for 42.47% and 21.26% of the variance, respectively (Figure 2). The three biological replicates for each developmental stage of *C. frutescens* peel samples clustered tightly together, indicating good reproducibility and reliability within each group. The large distances observed between the metabolite profiles of different growth stages reflect the distinct metabolic changes occurring during fruit development.

3.1.2. Screening for Differential Metabolites in the Pericarp of *C. frutescens* at Different Growth Periods

To further investigate the changes in metabolites during fruit color development in *C. frutescens*, UPLC-MS/MS was used to analyze peel samples from different growth stages. The differential metabolites between the stages were visualized using volcano plots (Figure 3). A total of 415 differential metabolites were identified between the immature stage (GR) and the semi-mature stage (OR), with 215 being upregulated and 200 being downregulated. Between the semi-mature stage (OR) and the mature stage (RE), 251 differential metabolites were found, with 146 being upregulated and 105 being downregulated.

Finally, between the mature stage (RE) and the immature stage (GR), 449 differential metabolites were identified, with 230 being upregulated and 219 being downregulated.

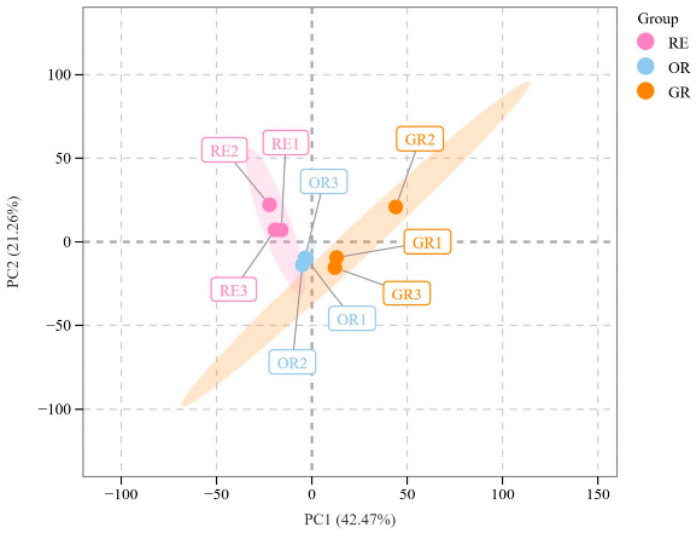


Figure 2. Metabolites of *C. frutescens* peel at different developmental stages according to principal component analysis (PCA). In the PCA plot, GR represents 50 days post-anthesis, OR represents 65 days post-anthesis, and RE represents 80 days post-anthesis.

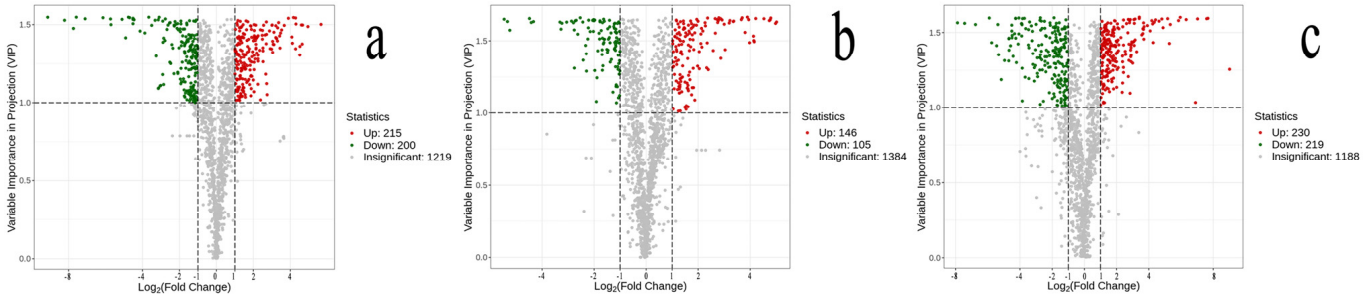


Figure 3. Volcanic diagram analysis of *C. frutescens* pericarp metabolites during different growth periods. In the volcano plots ((**a**) GR vs. OR; (**b**) OR vs. RE; (**c**) RE vs. GR), each point represents a metabolite. Green points indicate downregulated metabolites, red points indicate upregulated metabolites, and gray points represent metabolites with no significant difference. The x-axis represents the $\log_2$ fold change ($\log_2$FC) in relative metabolite levels between the two sample groups, with larger absolute values indicating greater differences. The y-axis represents the VIP score, where higher values indicate more significant differences and more reliable differential metabolites.

3.1.3. Identification of Flavonoid Compounds in the Pericarp of *C. frutescens* in Different Growth Periods

To further understand changes in flavonoid compounds during fruit color development, the flavonoids detected in *C. frutescens* peel samples at different growth stages were analyzed. A total of 43 flavonoid compounds were identified, including 14 flavonols, 11 dihydroflavonoids, 7 flavones, 4 chalcones, 4 flavanols, 2 dihydroflavonols, and 1 other flavonoid compound (Figure 4A). Among these, eight flavonoid metabolites showed significant differences, all of which exhibited a decreasing trend in content with increasing maturity. Eriodictyol, 5-O-p-coumaroyl quinic acid, and 3,4,2′,4′,6′-pentahydroxychalcone accumulated at higher levels during the immature stage (50 days post-anthesis). Pinobanksin, 2′,4,4′,6′-tetrahydroxychalcone, and naringenin were more abundant in the semi-mature stage (65 days post-anthesis). Epigallocatechin and phloretin-2′-O-glucoside accumulated more in the immature and semi-mature stages (50 and 65 days post-anthesis) than in the mature stage (80 days post-anthesis) (Figure 4B).

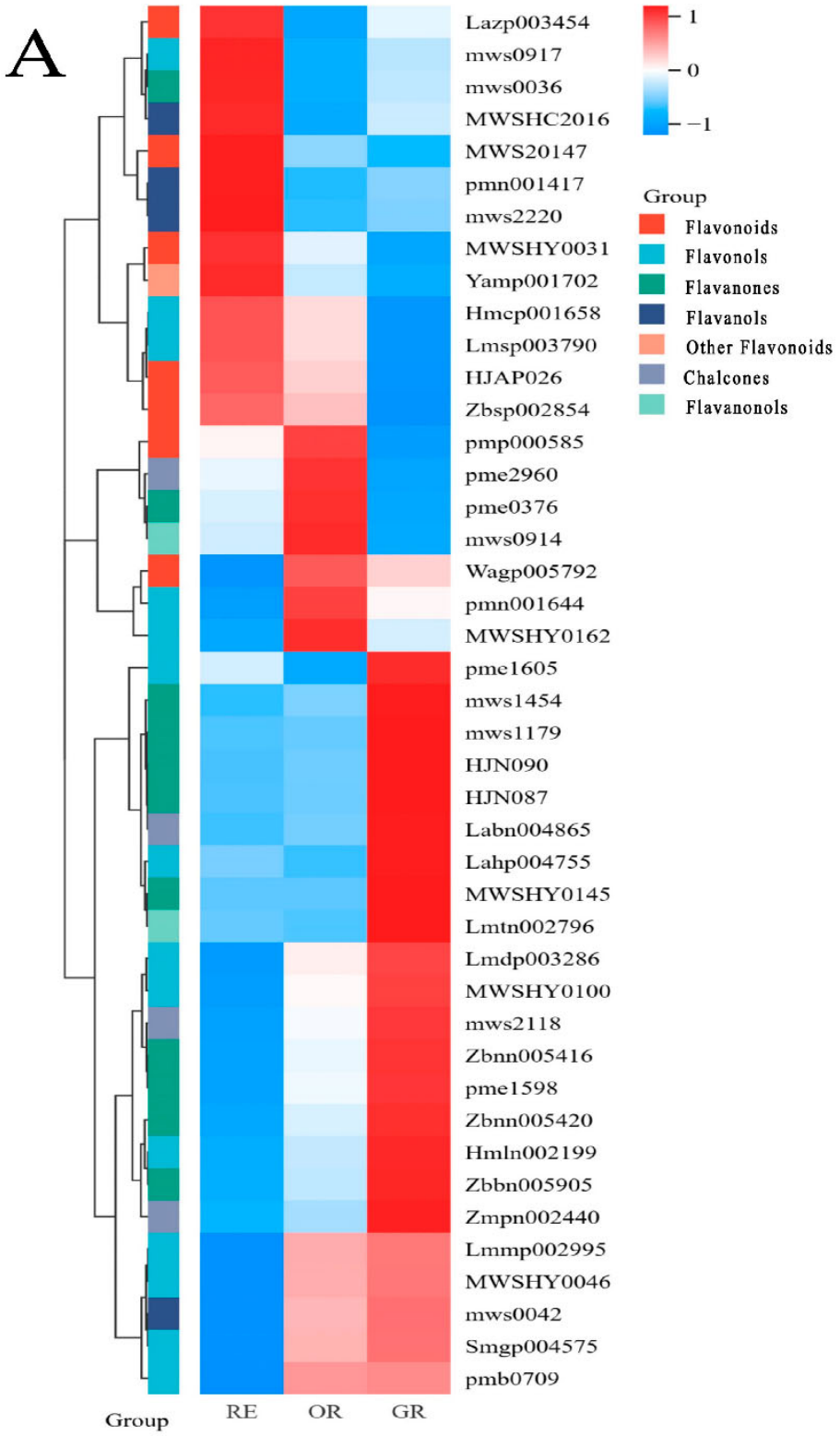


Figure 4. *Cont*.

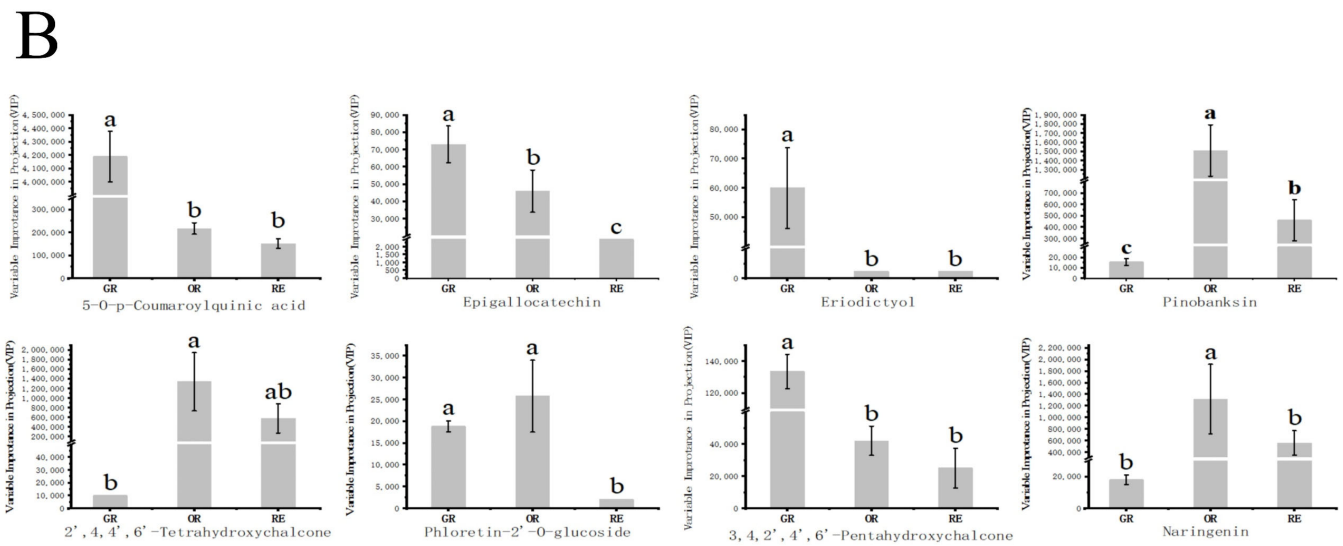


Figure 4. (**A**) Changes in the content of flavonoid metabolites at different growth stages of *C. frutescens*. (**B**) Analyses of the content of metabolites that change significantly at different growth stages (*C. frutescens*). In the heatmap, differential metabolites were selected based on a variable importance in projection (VIP) score ≥ 1 and an absolute value of Log_2 fold change ($|Log_2FC| \geq 1$). Red indicates increased metabolite levels, while blue indicates decreased levels. The right side shows the classification of the differential metabolites. In the bar chart, the y-axis represents the VIP score, indicating the degree of variation in metabolite levels, while the x-axis represents different growth stages. Significant differences between samples are marked by different letters, and error bars indicate the standard deviation of technical replicates.

3.2. Analysis of Pericarp Transcriptomics Data of C. frutescens at Different Growth Stages

To investigate the molecular mechanisms underlying changes in flavonoid content in *C. frutescens* peels over time, transcriptomic sequencing was performed on peel samples from three developmental stages. A total of nine *C. frutescens* fruit samples were sequenced after filtering, providing over 7 Gb of clean reads (data uploaded to the NCBI database BioProject ID: PRJNA1181927; access link: https://dataview.ncbi.nlm.nih.gov/object/PRJNA1181927?reviewer=l8g3skdieegg6f8qa8rrf6au8t; accessed on 5 November 2024). These clean reads were mapped to the reference genome (Zhangshugang_genome.fa.gz), with mapping rates exceeding 93%, a Q30 value above 96%, and GC content ranging from 43.1% to 43.86%. The biological replicates showed high correlation coefficients (greater than 0.8), meeting the requirements for subsequent analysis (Table 2). DESeq2 was used to perform differential expression analysis between the three groups of *C. frutescens* pericarp samples.

Table 2. Sequencing data and quality control.

Serial Number	Sample	Clean Base (Gb)	Q30 (%)	CG Content (%)	Reads Mapped (%)
1	RE1	8.49	96.71	43.1	94.14
2	RE2	8.38	96.82	43.24	94.08
3	RE3	10.3	96.96	43.22	94.34
4	OR1	10.19	96.87	43.13	94.43
5	OR2	7.49	97.05	43.15	94.36
6	OR3	11.97	97.14	43.37	93.18
7	GR1	7.19	96.8	43.6	94.36
8	GR2	8.23	96.8	43.35	93.83
9	GR3	9.92	96.77	43.86	94.44

A PCA analysis of differentially expressed genes (DEGs) showed that the three biological replicates from each developmental stage clustered tightly together, indicating

high reproducibility within each group. The large distances between samples from different stages reflected significant changes in gene expression over time (Figure 5A). A transcriptome analysis across different stages of *C. frutescens* was performed using the criteria of $|\log_2\text{Fold Change}| \geq 1$ and $p < 0.05$, identifying a total of 8928 DEGs. The number of DEGs between sample groups ranged from 3576 to 7033. In the GR vs. OR comparison, 5297 DEGs were identified (Figure 5C(a)), with 3330 being upregulated and 1967 being downregulated. In the OR vs. RE comparison, 3576 DEGs were identified (Figure 5C(b)), including 2371 upregulated and 1205 downregulated. In the RE vs. GR comparison, 7033 DEGs were identified (Figure 5C(c)), with 2540 being upregulated and 4493 being downregulated. The RE vs. GR comparison found the largest number of DEGs., while the fewest DEGs were identified in the OR vs. RE comparison. A total of 1040 DEGs were shared among all three comparisons (Figure 5B).

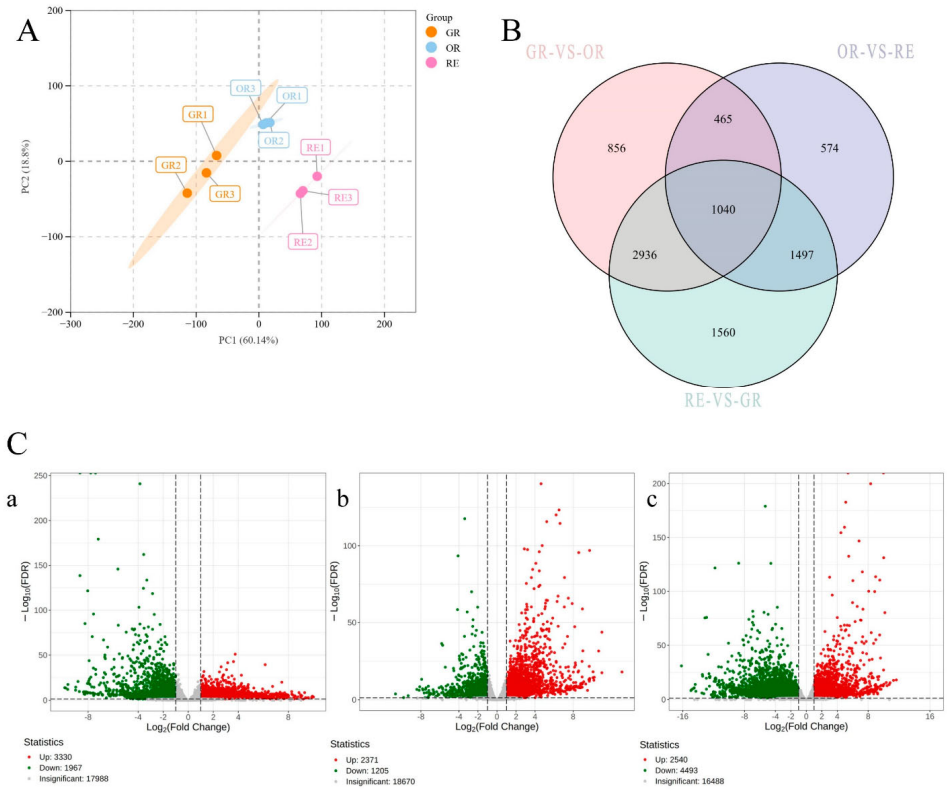


Figure 5. Transcriptomics data analysis of peppers pericarp at different growth stages. (**A**) Principal component analysis of pepper pericarp transcriptomes at different growth stages; (**B**) Venn plot analysis of pepper pericarp differential genes at different growth stages; (**C**) Volcano plot analysis of pepper pericarp differential genes at different growth stages. In the PCA plot, GR represents 50 days post-anthesis, OR represents 65 days post-anthesis, and RE represents 80 days post-anthesis, with three replicates per stage. In the Venn diagram, pink represents GR vs. OR, purple represents OR vs. RE, and green represents RE vs. GR. The non-overlapping regions represent unique genes specific to each comparison, while the overlapping regions represent shared differentially expressed genes (DEGs) among the comparisons. In the volcano plots ((**a**) GR vs. OR; (**b**) OR vs. RE; (**c**) RE vs. GR), each point represents a gene. Green points indicate downregulated genes, red points indicate upregulated genes, and gray points represent genes with no significant differences. The x-axis represents the fold change in gene expression, with larger absolute values indicating greater differences between the two sample groups. The y-axis represents the significance level of the differential genes, where higher values indicate more significant differences, making the identified DEGs more reliable.

3.3. Joint Transcriptome–Metabolome Analysis

Enrichment analysis was performed using hypergeometric tests to investigate the genes and metabolites in *C. frutescens* peels at different developmental stages. KEGG pathway enrichment analysis was conducted, and hypergeometric distribution tests were applied to the pathways. Differentially expressed genes (DEGs) were enriched in the flavonoid biosynthesis pathway in all three comparisons (pathway KO00941) (Figure 6). Based on this study, different species of *C. frutescens* exhibit variations in the specific types and amounts of flavonoid compounds [22], which may lead to differences in fruit color. Since the differential metabolites in all three comparisons were also enriched in the flavonoid biosynthesis pathway, we selected the flavonoid biosynthesis pathway (pathway KO00941) for further analysis.

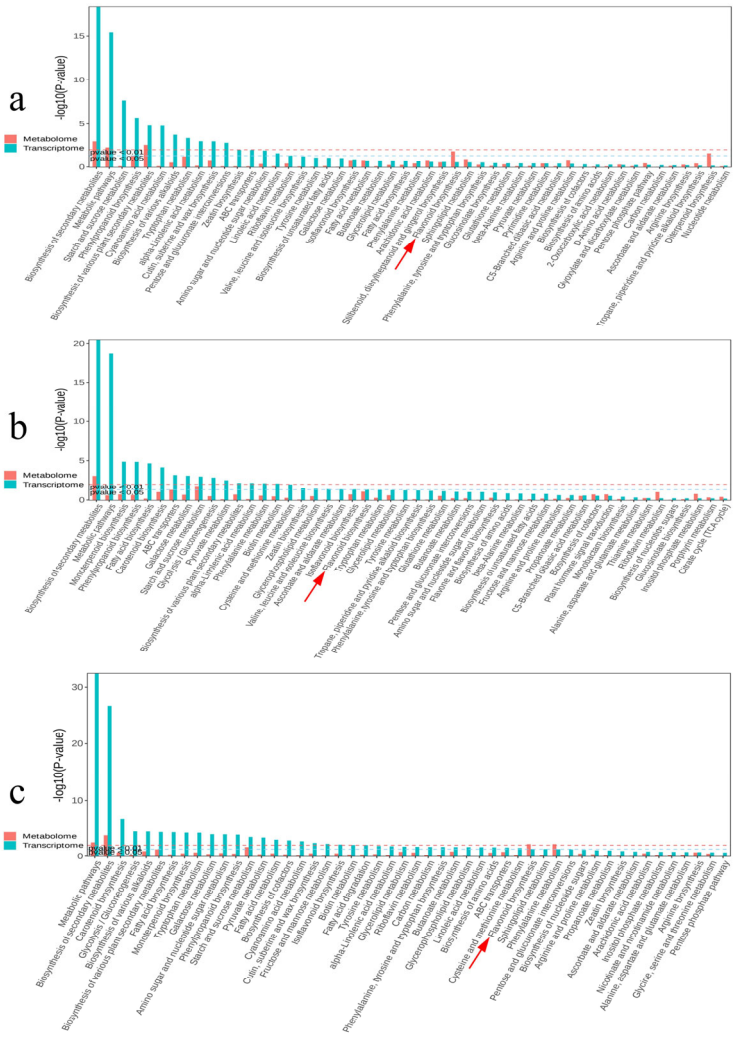


Figure 6. Combined analysis of transcriptome and metabolomics. KEGG enrichment bar plot. The x-axis represents the names of the KEGG pathways, while the y-axis indicates the significance of the enrichment *p*-values. In the KEGG enrichment analysis chart ((**a**) GR vs. OR; (**b**) OR vs. RE; (**c**) RE vs. GR), red bars represent metabolomic data, and green bars represent transcriptomic data.

A comparative analysis of the top 20 enriched KEGG pathways for DEGs across the three developmental stages of *C. frutescens* was conducted. By integrating the metabolomic and transcriptomic data of *C. frutescens*, we constructed a flavonoid biosynthesis pathway for the fruit (Figure 7A). Based on KEGG enrichment analysis, 28 key genes involved in flavonoid biosynthesis were identified (Figure 7C), including 13 *HCT*, 3 *E2.1.1.104*, 2 *C3'H*, 2 *CYP73A*, 2 *E5.5.1.6*, 2 *DFR*, 1 *ANS*, 1 *CHS*, 1 *CYP75B1* and 1 *FLS* genes. Most of these

genes were highly expressed in the immature fruit (50 days post-anthesis), while *DFR1* and *CYP75B1* showed higher expression in the semi-mature fruit (65 days post-anthesis). Only *ANS1* was highly expressed in the mature fruit (80 days post-anthesis). A Pearson correlation analysis was performed to assess the correlation between eight significantly different flavonoid metabolites and the expression levels of the 28 DEGs in the flavonoid biosynthesis pathway (Figure 7B). The results revealed 111 significant positive correlations and eight significant negative correlations. The analysis indicated that the *ANS*, *C3'H*, *CHS*, *CYP75B1*, *DFR*, *E2.1.1.104*, *FLS*, and *HCT* genes were significantly correlated with the identified flavonoid compounds showing differential expression.

Based on previous studies suggesting the involvement of the MBW complex in flavonoid biosynthesis [9,10], we ranked the top 100 differentially expressed genes by fold change ($|\mathrm{Log_2FC}|$) between the immature stage (50 days post-anthesis) and the mature stage (80 days post-anthesis), during which the most significant color changes occurred. Of these, eight transcription factors have been identified, of which three belong to the MYB family, four belong to the bHLH family, and one belongs to the WD family. A correlation analysis between these transcription factors and the significantly different flavonoid metabolites revealed a strong correlation (Figure 8A). Furthermore, correlation analysis between these eight transcription factors and the 28 key genes involved in flavonoid biosynthesis showed that with the exception of a negative correlation between *ANS1* and *DFR1*, all other transcription factors exhibited positive correlations (Figure 8B).

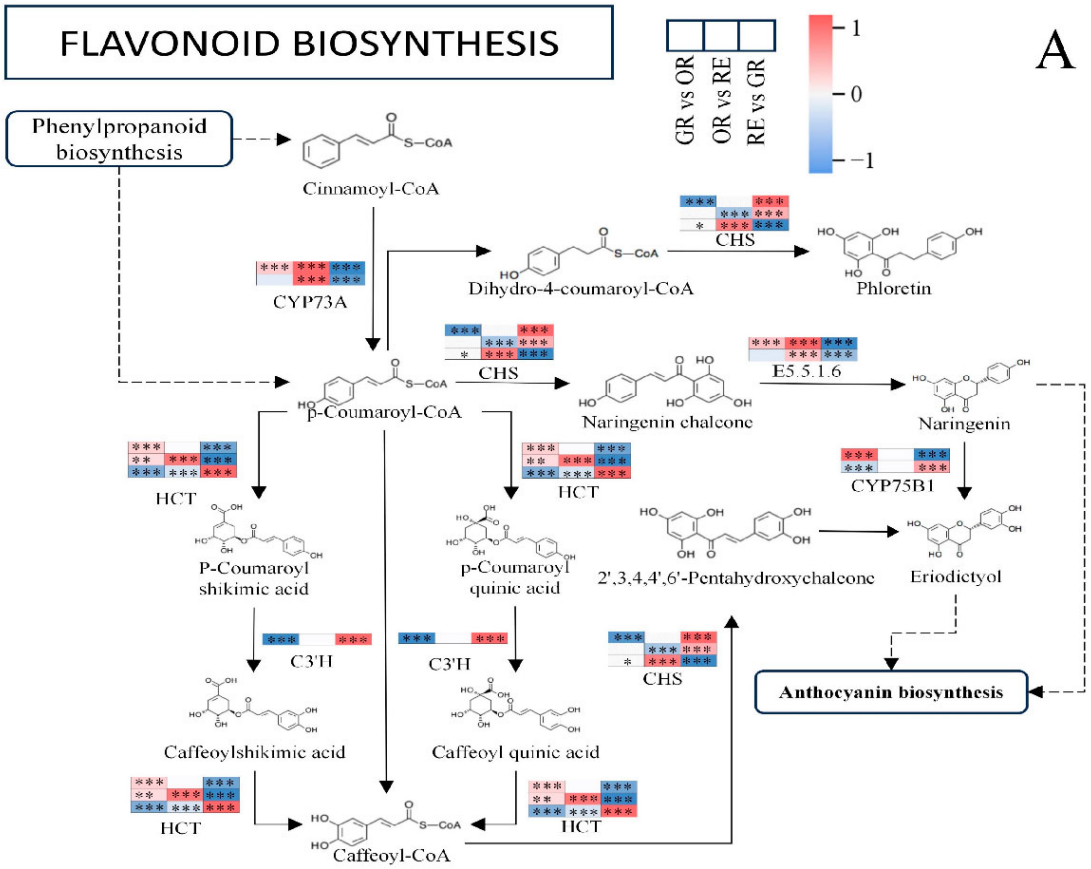


Figure 7. *Cont.*

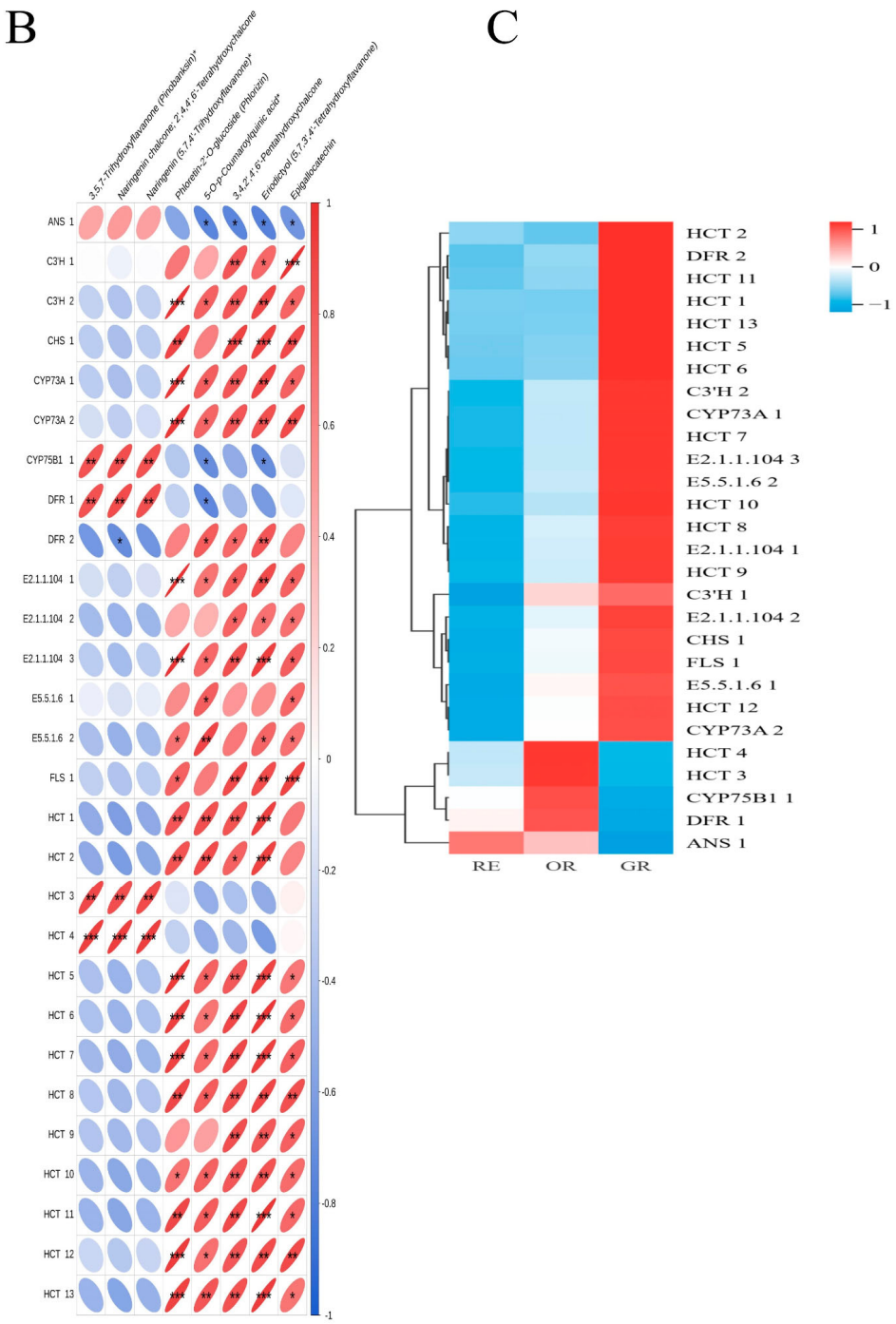


Figure 7. (**A**) Analysis of the flavonoid biosynthesis pathway visualized using a heatmap based on log2 fold changes. Asterisks indicate the significance level, with "*" $p < 0.05$, "**" $p < 0.01$, and "***" $p < 0.001$. Red indicates an increase in gene fold change, while blue indicates a decrease. Each line of data represents a transcript. (**B**) Correlation analysis between flavonoid biosynthesis genes and significantly different flavonoid metabolites. The y-axis shows the genes encoding flavonoid compounds, and the x-axis shows the significantly different flavonoid metabolites. Asterisks indicate the significance level, with "*" $p < 0.05$, "**" $p < 0.01$, and "***" $p < 0.001$. Red indicates positive correlations, and blue indicates negative correlations. (**C**) Gene expression analysis of flavonoid biosynthesis genes, using average FPKM values from three biological replicates. The x-axis represents the different developmental stages (GR: 50 days post-anthesis, OR: 65 days post-anthesis, RE: 80 days post-anthesis), and the y-axis shows the gene names.

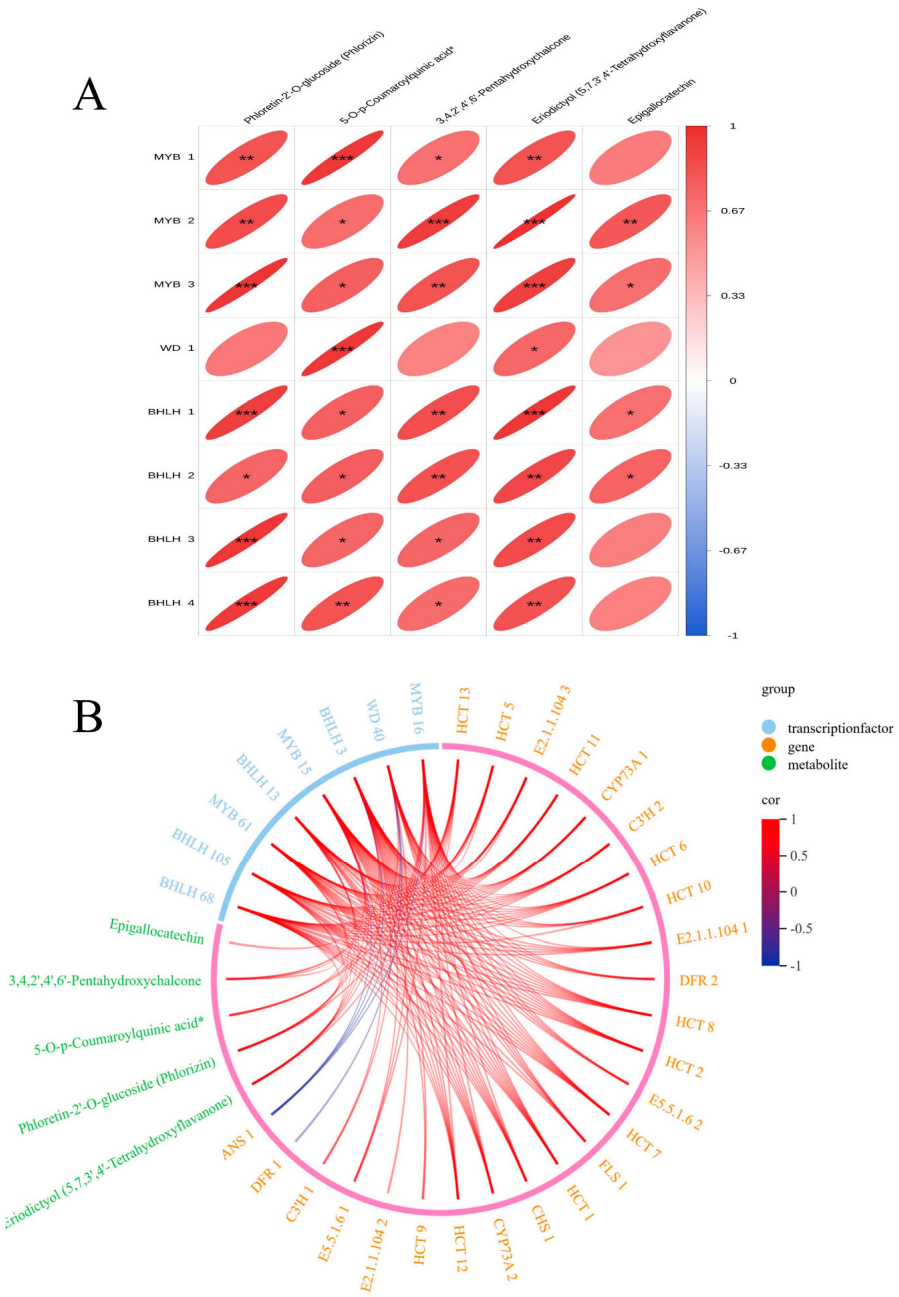


Figure 8. (**A**) Correlation analysis between transcription factors and significantly different flavonoid metabolites based on Pearson correlation. The y-axis represents the transcription factor names, and the x-axis shows significantly different flavonoid metabolites. Asterisks indicate the significance level, with "*" $p < 0.05$, "**" $p < 0.01$, and "***" $p < 0.001$. (**B**) Correlation analysis between transcription factors and genes encoding flavonoid biosynthesis. Blue represents transcription factors, green represents significantly different flavonoid metabolites, and orange represents flavonoid biosynthesis genes. Red lines indicate positive correlations, and blue lines indicate negative correlations.

To further understand flavonoid biosynthesis, we randomly selected nine core genes involved in flavonoid biosynthesis and eight potentially related genes for qRT-PCR analysis to assess their expression changes across different developmental stages of the fruit. This analysis also served to validate the transcriptomic data. The qRT-PCR results showed that the expression trends of the nine selected genes were consistent with the FPKM values from the transcriptomic analysis, further confirming the accuracy and reliability of the transcriptomic data (Figure 9A). In addition, a general decrease in relative expression levels

as the chili fruit matured was observed in the qRT-PCR results for the transcription factors (Figure 9B).

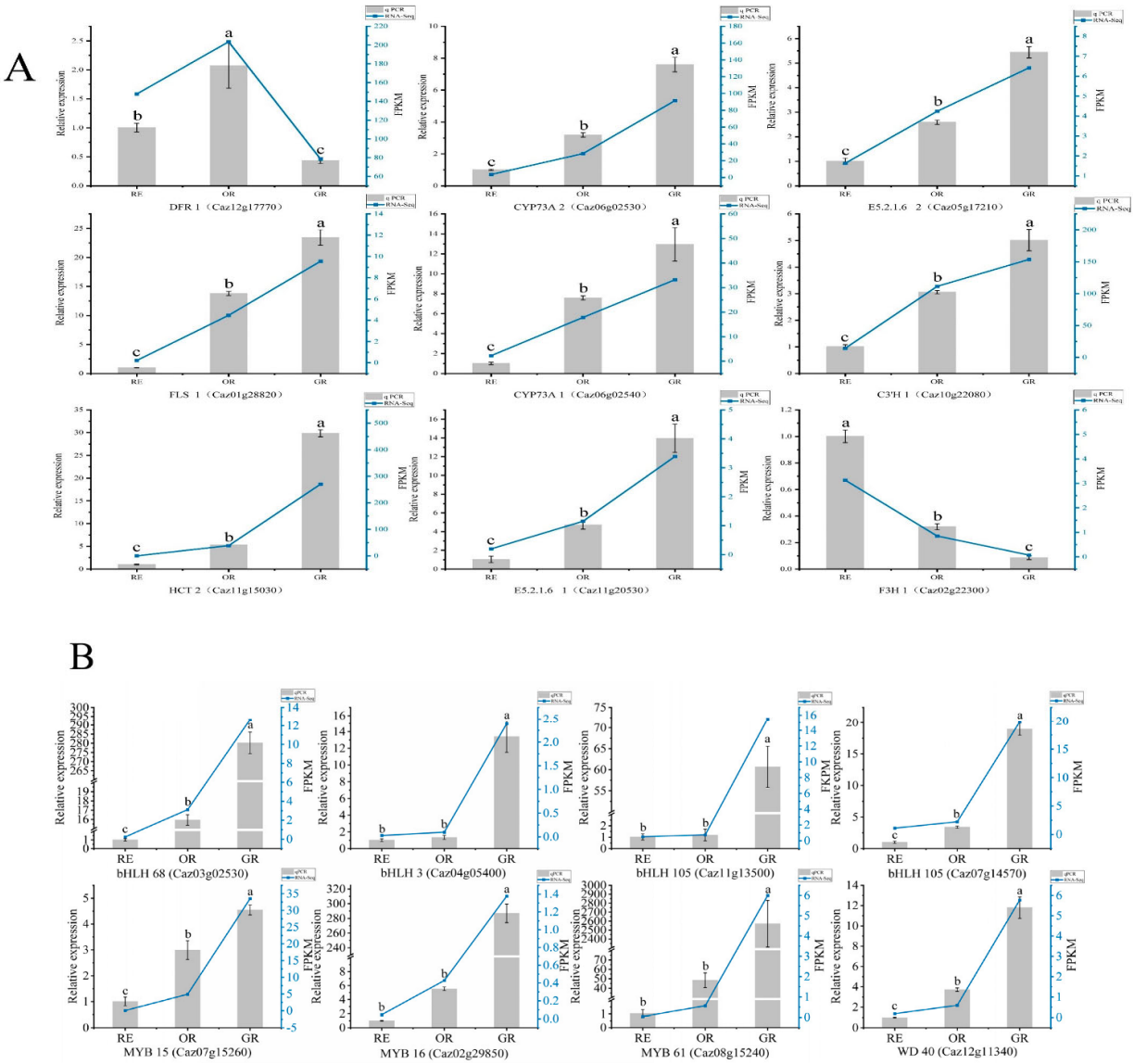


Figure 9. (**A**) Trend analysis comparing transcriptomic data and qRT-PCR results. The x-axis represents different developmental stages (GR: 50 days post-anthesis, OR: 65 days post-anthesis, RE: 80 days post-anthesis). The left y-axis (black) represents relative expression, and the right y-axis (blue) represents FPKM values. Error bars represent technical replicate errors. qPCR significance is indicated by a change in lowercase letters (**B**) Expression pattern analysis of transcription factors. The x-axis represents different developmental stages (GR: 50 days post-anthesis, OR: 65 days post-anthesis, RE: 80 days post-anthesis), the left y-axis (black) represents relative expression, and the right y-axis (blue) represents FPKM values. Error bars represent technical replicate errors. qPCR significance is indicated by a change in lowercase letters.

4. Discussion

Fruit color was often considered an important quality trait [23], with studies showing that changes in the accumulation of flavonoids in plants frequently led to changes in fruit color [24]. Flavonoids were key secondary metabolites widely distributed in plants, including vegetables and fruits [25–27]. Flavonoid biosynthesis has long been a focus of plant physiology research, as flavonoids play an important role in several plant physiological processes [28]. Studies on Solanaceae species have demonstrated a strong correlation be-

tween flavonoid accumulation and fruit color transition [24,29,30]. In a recent survey of chrysanthemum ("Fencui" cultivar), it was also reported that *CmMYB012* could regulate *CmFNS* to inhibit the biosynthesis of flavonoids, which ultimately affects the flower color of the plant [31]. In this study, we analyzed *C. frutescens* fruit at different developmental stages using metabolomic and transcriptomic data. Our results showed that flavonoid compounds and the genes encoding flavonoid biosynthesis change as the fruit develops. A KEGG enrichment analysis of transcriptomics and metabolomics data showed that both were enriched in the flavonoid metabolic pathway; based on previous research, we hypothesized that flavonoid compounds in the peel degrade over time, leading to the color transition of the fruit from green to red.

A metabolomic analysis identified 43 flavonoid metabolites in the peel of *C. frutescens*, comprising seven subcategories, indicating a rich presence of flavonoid compounds in *C. frutescens* peels. Among the detected flavonoids, significant changes were observed in flavonols and dihydroflavonoids during fruit development. Notably, 3,5,7-trihydroxyflavanone (pinobanksin), naringenin chalcone, naringenin, phlorizin, 5-O-p-coumaroylquinic acid, 3,4,2′,4′,6′-pentahydroxychalcone, eriodictyol, and epigallocatechin exhibited the most pronounced differences. In plants, flavonoids accumulated in various ways and were key biomolecules influencing pigmentation, often found in epidermal tissues [32,33]. In this study, the significantly different flavonoid compounds showed a declining trend in content as the fruit matured, suggesting that flavonoids may gradually degrade into other substances, contributing to color changes during fruit development. This finding aligns with the results of Allwood et al.'s [34] study on blackcurrant (*Ribes nigrum*). There were clear differences in both the type and content of metabolites at various stages of *C. frutescens* development, with the most notable changes occurring as the fruit transitioned from the orange stage (65 days post-anthesis) to the red stage (80 days post-anthesis). This observation was consistent with the findings of Heng et al. [35], who reported significant metabolite content differences in *C. frutescens* between the semi-mature and mature stages. Based on these results, we hypothesized that the breakdown and transformation of these metabolites primarily occur during the transition from the semi-mature to the mature stages.

1. An RNA-Seq analysis identified 28 key genes involved in the core flavonoid biosynthesis pathway. These genes were similar to the flavonoid biosynthesis genes involved in peel coloration in melon [36], although *4CL*, *IFS*, and *UFGT* did not show significant differential expression in this study, which we hypothesized may be due to interspecies differences. *CHS* was a crucial enzyme in the synthesis of flavonoid compounds in plants and played a vital role in producing flavonoid derivatives and supporting plant growth and development [37–39]. In our study, p-coumaroyl-CoA was catalyzed by *CHS* to produce naringenin chalcone. Similarly, another study found a significant increase in anthocyanin content during pepper maturation, which was associated with the color transition from green to red [3]. Their study highlighted the upregulation of genes involved in anthocyanin biosynthesis, such as *CHS* and *DFR*, highlighting the role of flavonoids in pepper coloration at later stages of fruit development. Studies on *Marchantia polymorpha* have shown that PabHLH1 can catalyze the synthesis of flavonoids [40], while CmMYB012 in *chrysanthemum* negatively regulates flavonoids [31]. Studies on *Medicago* have also mentioned that MtWD40 can regulate the production of anthocyanins [41]. In this study, we screened a total of eight MBW complex genes (MYB–bHLH–WD repeat) by Pearson correlation coefficient and analyzed their expression patterns. We found that all eight genes showed high expression during the early growth of plants and decreased expression as the plants grew. A correlation analysis of the eight genes screened and the flavonoid metabolites with

significant differences found that they were all positively correlated. We speculate that the regulation of flavonoid biosynthesis may be involved in these eight genes.

Furthermore, studies on other fruit-bearing plants, such as grapes (*Vitis vinifera*) and blueberries (*Vaccinium* spp.), have shown similar patterns of flavonoid accumulation. In grapes, anthocyanin content significantly increased with fruit maturation and led to a color shift from red to purple [42]. Similarly, this study reported that the rise in anthocyanin levels caused blueberries to transition from green to deep blue, with anthocyanin content peaking at full fruit maturity [43]. However, when comparing our findings with those of other studies on *C. frutescens*, certain differences emerge. For instance, the specific types and quantities of flavonoid compounds varied across different pepper species, potentially leading to distinct fruit colors [22]. This suggests that while the general trend of increased flavonoid content associated with fruit maturation was conserved across *C. frutescens*, the specific changes in flavonoid composition and their effects on fruit color may vary between different pepper varieties.

While this study provided valuable insights, several limitations should be acknowledged. First, our research focused on a single *C. frutescens* variety. Given the genetic diversity within the Capsicum genus, repeating this study across different pepper varieties would help determine whether the observed patterns of flavonoid accumulation and color changes were consistent. This would aid in identifying any varietal differences and broaden our understanding of flavonoid compounds in *C. frutescens*. On the other hand, this study was carried out under controlled environmental conditions. Flavonoid biosynthesis and fruit pigmentation can be significantly influenced by factors such as light intensity, temperature, and soil nutrients [44]. Future research should explore the impact of different environmental conditions on flavonoid accumulation and fruit coloration in *C. frutescens*. Such studies could provide insights into how environmental stressors regulate flavonoid pathways and affect fruit quality. Additionally, our study did not examine potential interactions between flavonoids and other metabolites that may influence fruit color. Metabolites such as carotenoids and chlorophyll also affect fruit color and may interact with flavonoids in complex ways [45]. Finally, the nutritional and health benefits of flavonoids were well established, with numerous studies highlighting their antioxidant, anti-inflammatory, and anticancer properties [46]. Understanding the changes in flavonoid content in chili fruits could guide efforts to enhance their nutritional and economic value.

5. Conclusions

During the development of *C. frutescens* fruit from the immature to mature stages, we identified 28 key genes involved in flavonoid biosynthesis and 8 additional genes with potential regulatory roles. Eight flavonoid compounds that exhibited significant changes during fruit growth were also identified. Except for the negative correlation between *ANS1* and *DFR1*, all other gene–metabolite correlations were positive, indicating their important roles in the maturation process of *C. frutescens* fruit. In addition, the eight screened transcription factors all exhibited high expression levels during the early growth stage of the plant. Combined with the changing trends of flavonoid metabolites, we speculate that these transcription factors may be involved in regulating the biosynthesis of flavonoid compounds and that changes in the content of flavonoid compounds in the plant body have led to changes in the color of the *C. frutescens* fruit pericarp. These findings contributed to a broader understanding of flavonoid biosynthesis and its dynamic changes in *C. frutescens*.

Author Contributions: Conceptualization, Y.Y. (Yinxin Yang), Q.C., L.L., Z.S. and W.L.; data curation, Y.Y. (Yinxin Yang), Q.C. and Z.S.; formal analysis, Y.Y. (Yinxin Yang); funding acquisition, Z.S.;

investigation, Y.Y. (Yinxin Yang), Q.C., X.W. and Y.Y. (Yanbo Yang); methodology, Y.Y. (Yinxin Yang), Y.Y. (Yanbo Yang) and Z.S.; project administration, L.L. and Z.S.; resources, Y.Y. (Yinxin Yang), X.W. and L.L.; software, Y.Y. (Yinxin Yang); supervision, X.W. and W.L.; validation, Y.Y. (Yinxin Yang); visualization, Y.Y. (Yinxin Yang) and Q.C.; writing—original draft, Y.Y. (Yinxin Yang); writing—review and editing, Y.Y. (Yinxin Yang), Z.S. and W.L. All authors have read and agreed to the published version of the manuscript.

Funding: This work was funded by the Key Research and Development Program of Yunnan Province (202403AP140045; 202403AP140026).

Data Availability Statement: All data are available in the main text. The transcriptome sequence data have been uploaded to the NCBI database (BioProject ID: PRJNA1181927; access link: https://dataview.ncbi.nlm.nih.gov/object/PRJNA1181927?reviewer=l8g3skdieegg6f8qa8rrf6au8t; accessed on 5 November 2024).

Acknowledgments: We would like to thank Zhenghai Sun for editing this document and Qihang Cai, Xuan Wang, and Yanbo Yang for their technical assistance.

Conflicts of Interest: The authors declare no conflicts of interest.

References

1. Timberlake, C.F. Plant pigments for colouring food. *Nutr. Bull.* **1989**, *14*, 113–125. [CrossRef]
2. Facteau, T.; Chestnut, N.; Rowe, K. Relationship between fruit weight, firmness, and leaf/fruit ratio in Lambert and Bing sweet cherries. *Can. J. Plant Sci.* **1983**, *63*, 763–765. [CrossRef]
3. Lightbourn, G.J.; Griesbach, R.J.; Novotny, J.A.; Clevidence, B.A.; Rao, D.D.; Stommel, J.R. Effects of anthocyanin and carotenoid combinations on foliage and immature fruit color of *Capsicum annuum* L. *J. Hered.* **2008**, *99*, 105–111. [CrossRef] [PubMed]
4. Ferrer, J.-L.; Austin, M.; Stewart Jr, C.; Noel, J. Structure and function of enzymes involved in the biosynthesis of phenylpropanoids. *Plant Physiol. Biochem.* **2008**, *46*, 356–370. [CrossRef]
5. Chen, W.; Gao, Y.; Xie, W.; Gong, L.; Lu, K.; Wang, W.; Li, Y.; Liu, X.; Zhang, H.; Dong, H. Genome-wide association analyses provide genetic and biochemical insights into natural variation in rice metabolism. *Nat. Genet.* **2014**, *46*, 714–721. [CrossRef]
6. Cheng, A.X.; Han, X.J.; Wu, Y.F.; Lou, H.X. The function and catalysis of 2-oxoglutarate-dependent oxygenases involved in plant flavonoid biosynthesis. *Int. J. Mol. Sci.* **2014**, *15*, 1080–1095. [CrossRef] [PubMed]
7. Wang, D.; Wang, K.; Sun, S.; Yan, P.; Lu, X.; Liu, Z.; Li, Q.; Li, L.; Gao, Y.; Liu, J. Transcriptome and Metabolome Analysis Reveals Salt-Tolerance Pathways in the Leaves and Roots of ZM-4 (Malus zumi) in the Early Stages of Salt Stress. *Int. J. Mol. Sci.* **2023**, *24*, 3638. [CrossRef] [PubMed]
8. Forkmann, G. Flavonoids as Flower Pigments; The Formation of the Natural Spectrum and its Extension by Genetic Engineering. *Plant Breed.* **1991**, *106*, 1–26. [CrossRef]
9. Koes, R.; Verweij, W.; Quattrocchio, F. Flavonoids: A colorful model for the regulation and evolution of biochemical pathways. *Trends Plant Sci.* **2005**, *10*, 236–242. [CrossRef] [PubMed]
10. Dubos, C.; Stracke, R.; Grotewold, E.; Weisshaar, B.; Martin, C.; Lepiniec, L. MYB transcription factors in Arabidopsis. *Trends Plant Sci.* **2010**, *15*, 573–581. [CrossRef] [PubMed]
11. Liu, Y.; Lv, J.; Liu, Z.; Wang, J.; Yang, B.; Chen, W.; Ou, L.; Dai, X.; Zhang, Z.; Zou, X. Integrative analysis of metabolome and transcriptome reveals the mechanism of color formation in pepper fruit (*Capsicum annuum* L.). *Food Chem.* **2020**, *306*, 125629. [CrossRef] [PubMed]
12. Tang, B.; Li, L.; Hu, Z.; Chen, Y.; Tan, T.; Jia, Y.; Xie, Q.; Chen, G. Anthocyanin accumulation and transcriptional regulation of anthocyanin biosynthesis in purple pepper. *J. Agric. Food Chem.* **2020**, *68*, 12152–12163. [CrossRef] [PubMed]
13. Howard, L.R.; Talcott, S.T.; Brenes, C.H.; Villalon, B. Changes in phytochemical and antioxidant activity of selected pepper cultivars (*Capsicum* species) as influenced by maturity. *J. Agric. Food Chem.* **2000**, *48*, 1713–1720. [CrossRef] [PubMed]
14. Dozmorov, M.G. Epigenomic annotation-based interpretation of genomic data: From enrichment analysis to machine learning. *Bioinformatics* **2017**, *33*, 3323–3330. [CrossRef] [PubMed]
15. Shu, P.; Zhang, Z.; Wu, Y.; Chen, Y.; Li, K.; Deng, H.; Zhang, J.; Zhang, X.; Wang, J.; Liu, Z. A comprehensive metabolic map reveals major quality regulations in red-flesh kiwifruit (*Actinidia chinensis*). *New Phytol.* **2023**, *238*, 2064–2079. [CrossRef] [PubMed]
16. Kanehisa, M.; Furumichi, M.; Sato, Y.; Kawashima, M.; Ishiguro-Watanabe, M. KEGG for taxonomy-based analysis of pathways and genomes. *Nucleic Acids Res.* **2023**, *51*, D587–D592. [CrossRef] [PubMed]
17. Liao, Y.; Smyth, G.K.; Shi, W. featureCounts: An efficient general purpose program for assigning sequence reads to genomic features. *Bioinformatics* **2014**, *30*, 923–930. [CrossRef]

18. Love, M.I.; Huber, W.; Anders, S. Moderated estimation of fold change and dispersion for RNA-seq data with DESeq. *Genome Biol.* **2014**, *15*, 1–21. [CrossRef] [PubMed]
19. Varet, H.; Brillet-Guéguen, L.; Coppée, J.-Y.; Dillies, M.-A. SARTools: A DESeq2-and EdgeR-based R pipeline for comprehensive differential analysis of RNA-Seq data. *PLoS ONE* **2016**, *11*, e0157022. [CrossRef] [PubMed]
20. Yang, L.; Wang, P.; Chen, J. 2dGBH: Two-dimensional group Benjamini–Hochberg procedure for false discovery rate control in two-way multiple testing of genomic data. *Bioinformatics* **2024**, *40*, btae035. [CrossRef]
21. Livak, K.J.; Schmittgen, T.D. Analysis of relative gene expression data using real-time quantitative PCR and the $2-\Delta\Delta CT$ method. *Methods* **2001**, *25*, 402–408. [CrossRef]
22. Wahyuni, Y.; Ballester, A.R.; Sudarmonowati, E.; Bino, R.J.; Bovy, A.G. Metabolite biodiversity in pepper (*Capsicum*) fruits of thirty-two diverse accessions: Variation in health-related compounds and implications for breeding. *Phytochemistry* **2011**, *72*, 1358–1370. [CrossRef] [PubMed]
23. Bashir, M.A.; Alvi, A.M.; Khan, K.A.; Rehmani, M.I.A.; Ansari, M.J.; Atta, S.; Ghramh, H.A.; Batool, T.; Tariq, M. Role of pollination in yield and physicochemical properties of tomatoes (*Lycopersicon esculentum*). *Saudi J. Biol. Sci.* **2018**, *25*, 1291–1297. [CrossRef] [PubMed]
24. Kang, S.I.; Hwang, I.; Goswami, G.; Jung, H.J.; Nath, U.K.; Yoo, H.J.; Lee, J.M.; Nou, I.S. Molecular Insights Reveal Psy1, SGR, and SlMYB12 Genes are Associated with Diverse Fruit Color Pigments in Tomato (*Solanum lycopersicum* L.). *Molecules* **2017**, *22*, 2180. [CrossRef] [PubMed]
25. Wang, H.J.; Pao, L.H.; Hsiong, C.H.; Shih, T.Y.; Lee, M.S.; Hu, O.Y. Dietary flavonoids modulate CYP2C to improve drug oral bioavailability and their qualitative/quantitative structure-activity relationship. *Aaps J.* **2014**, *16*, 258–268. [CrossRef] [PubMed]
26. Khoo, B.Y.; Chua, S.L.; Balaram, P. Apoptotic effects of chrysin in human cancer cell lines. *Int. J. Mol. Sci.* **2010**, *11*, 2188–2199. [CrossRef] [PubMed]
27. Liu, J.; Li, C.; Ding, G.; Quan, W. Artificial intelligence assisted ultrasonic extraction of total flavonoids from *Rosa sterilis*. *Molecules* **2021**, *26*, 3835. [CrossRef] [PubMed]
28. Liu, W.; Feng, Y.; Yu, S.; Fan, Z.; Li, X.; Li, J.; Yin, H. The Flavonoid Biosynthesis Network in Plants. *Int. J. Mol. Sci.* **2021**, *22*, 12824. [CrossRef] [PubMed]
29. Zhang, Y.; Ma, C.; Liu, C.; Wei, F. Luteolin attenuates doxorubicin-induced cardiotoxicity by modulating the PHLPP1/AKT/Bcl-2 signalling pathway. *PeerJ* **2020**, *8*, e8845. [CrossRef] [PubMed]
30. Dymarska, M.; Janeczko, T.; Kostrzewa-Suslow, E. Glycosylation of Methoxylated Flavonoids in the Cultures of Isaria fumosorosea KCH J2. *Molecules* **2018**, *23*, 2578. [CrossRef] [PubMed]
31. Zhou, L.-J.; Geng, Z.; Wang, Y.; Wang, Y.; Liu, S.; Chen, C.; Song, A.; Jiang, J.; Chen, S.; Chen, F. A novel transcription factor CmMYB012 inhibits flavone and anthocyanin biosynthesis in response to high temperatures in chrysanthemum. *Hortic. Res.* **2021**, *8*, 248. [CrossRef]
32. Adato, A.; Mandel, T.; Mintz-Oron, S.; Venger, I.; Levy, D.; Yativ, M.; Domínguez, E.; Wang, Z.; De Vos, R.C.; Jetter, R.; et al. Fruit-surface flavonoid accumulation in tomato is controlled by a SlMYB12-regulated transcriptional network. *PLoS Genet.* **2009**, *5*, e1000777. [CrossRef] [PubMed]
33. Zhou, X.-J.; Hu, C.-T.; Yan, Y.; Wu, S.; Wang, J. A novel microfluidic aqueous two-phase system with immobilized enzyme enhances cyanidin-3-O-glucoside content in red pigments from mulberry fruits. *Biochem. Eng. J.* **2020**, *158*. [CrossRef]
34. Allwood, J.W.; Woznicki, T.L.; Xu, Y.; Foito, A.; Aaby, K.; Sungurtas, J.; Freitag, S.; Goodacre, R.; Stewart, D.; Remberg, S.F.; et al. Application of HPLC-PDA-MS metabolite profiling to investigate the effect of growth temperature and day length on blackcurrant fruit. *Metabolomics* **2019**, *15*, 12. [CrossRef] [PubMed]
35. Heng, Z.; Xu, X.; Xu, X.; Li, Y.; Wang, H.; Huang, W.; Yan, S.; Li, T. Integrated transcriptomic and metabolomic analysis of *C frutescens* fruits provides new insight into the regulation of the branched chain esters and capsaicin biosynthesis. *Food Res. Int.* **2023**, *169*, 112856. [CrossRef] [PubMed]
36. Zhang, A.; Zheng, J.; Chen, X.; Shi, X.; Wang, H.; Fu, Q. Comprehensive Analysis of Transcriptome and Metabolome Reveals the Flavonoid Metabolic Pathway Is Associated with Fruit Peel Coloration of Melon. *Molecules* **2021**, *26*, 2830. [CrossRef] [PubMed]
37. Aksamit-Stachurska, A.; Korobczak-Sosna, A.; Kulma, A.; Szopa, J. Glycosyltransferase efficiently controls phenylpropanoid pathway. *BMC Biotechnol.* **2008**, *8*, 25. [CrossRef] [PubMed]
38. Kong, X.; Khan, A.; Li, Z.; You, J.; Munsif, F.; Kang, H.; Zhou, R. Identification of chalcone synthase genes and their expression patterns reveal pollen abortion in cotton. *Saudi J. Biol. Sci.* **2020**, *27*, 3691–3699. [CrossRef] [PubMed]
39. Wang, Z.; Yu, Q.; Shen, W.; El Mohtar, C.A.; Zhao, X.; Gmitter, F.G., Jr. Functional study of CHS gene family members in citrus revealed a novel CHS gene affecting the production of flavonoids. *BMC Plant Biol.* **2018**, *18*, 189. [CrossRef] [PubMed]
40. Zhao, Y.; Zhang, Y.-Y.; Liu, H.; Zhang, X.-S.; Ni, R.; Wang, P.-Y.; Gao, S.; Lou, H.-X.; Cheng, A.-X. Functional characterization of a liverworts bHLH transcription factor involved in the regulation of bisbibenzyls and flavonoids biosynthesis. *BMC Plant Biol.* **2019**, *19*, 1–13. [CrossRef]

41. Pang, Y.; Wenger, J.P.; Saathoff, K.; Peel, G.J.; Wen, J.; Huhman, D.; Allen, S.N.; Tang, Y.; Cheng, X.; Tadege, M. A WD40 repeat protein from Medicago truncatula is necessary for tissue-specific anthocyanin and proanthocyanidin biosynthesis but not for trichome development. *Plant Physiol.* **2009**, *151*, 1114–1129. [CrossRef]
42. Castellarin, S.D.; Matthews, M.A.; Di Gaspero, G.; Gambetta, G.A. Water deficits accelerate ripening and induce changes in gene expression regulating flavonoid biosynthesis in grape berries. *Planta* **2007**, *227*, 101–112. [CrossRef] [PubMed]
43. Prior, R.; Cao, G.; Martin, A.; Sofi, E.; Mcewen, J.; O'Brien, C.; Lischner, N.; Ehlenfeldt, M.; Kalt, W.; Krewer, G. Antioxidant capacity as influenced by total phenolic and anthocyanin content, maturity, and variety of *Vaccinium* species. *J. Agric. Food Chem.* **1998**, *46*, 2686–2693. [CrossRef]
44. Zoratti, L.; Karppinen, K.; Luengo Escobar, A.; Häggman, H.; Jaakola, L. Light-controlled flavonoid biosynthesis in fruits. *Front. Plant Sci.* **2014**, *5*, 534. [CrossRef] [PubMed]
45. Ralley, L.; Enfissi, E.M.; Misawa, N.; Schuch, W.; Bramley, P.M.; Fraser, P.D. Metabolic engineering of ketocarotenoid formation in higher plants. *Plant J.* **2004**, *39*, 477–486. [CrossRef] [PubMed]
46. Zanoaga, O.; Braicu, C.; Jurj, A.; Rusu, A.; Buiga, R.; Berindan-Neagoe, I. Progress in Research on the Role of Flavonoids in Lung Cancer. *Int. J. Mol. Sci.* **2019**, *20*, 4291. [CrossRef]

Disclaimer/Publisher's Note: The statements, opinions and data contained in all publications are solely those of the individual author(s) and contributor(s) and not of MDPI and/or the editor(s). MDPI and/or the editor(s) disclaim responsibility for any injury to people or property resulting from any ideas, methods, instructions or products referred to in the content.